Constitutive model for 2D analysis of iso-kinematic frictional contact problems

João B. de Aguiar
Sistemas Mecânicos, Escola Politécnica, USP, SP – Brazil
Renato T. Vargas
Consultor, NEP Consultoria, São Paulo, SP – Brazil

Abstract

During contact between two surfaces, a part the normal pressure between the surfaces, tangential forces that involve dissipative phenomena related to friction, occur. Modeling the interface friction involves adherence and slipping. This last effect may include evolution equations considering displacement hardening with isotropic or kinematic surfaces involved. Isotropic conditions are generally considered, what may be inadequate to cyclic loadings. Kinematic models address this difficulty and should handle these cases better. Here a kinematic model is formulated, developed and implemented for two-dimensional problems. Corotational measures are used in the setting of the constitutive incremental equations for quasi-static conditions, without thermal coupling. An implicit numerical scheme is used to develop the solution procedure. A few cyclic cases are used to verify the model, followed by an application problem. Results are compared to available solutions with acceptable agreement.

Keywords: friction, constitutive equation, kinematic modeling

1 Introduction

Frictional contact between surfaces is an area of intense research, with several applications in mechanics. Many phenomena occur in the interface, and modeling of them is quite difficult. Solution to a few, but yet very important set of problems has been devised, with construction of some models. Discretization to allow finite element analysis is the another factor that requires special care [1].

In most of the cases, interface friction is modeled using Coulomb law, or modifications of this law. As a first order approach to the understanding of interface phenomena, this law is very significative. But it fails in many aspects, mostly when very large interface pressures are present. Therefore models with more amplitude and generality are required. Elasto-plastic models are of great importance, as they set a parallel to the development of friction models. Here this will be followed as well.

Mechanics of Solids in Brazil 2007, Marcílio Alves & H.S. da Costa Mattos (Editors)
Brazilian Society of Mechanical Sciences and Engineering, ISBN 978-85-85769-30-7

2 Model

Curnier [2] developed systematic studies to compare and find analogies between models in elastoplasticiy and friction. He addressed some topics:

2.1 Additive decomposition

Courtney-Pratt and Eisner [3] studied the relative motion of two surfaces, one of them moving, a disk, relative to another one, fixed, both made up of polished platinum, both subjected to tangential forces. Obtained results, presented in Figure 1, show the approximately linear relationship between the tangential component, affected of the Constant normal, and the tangential relative displacement, during both, loading and unloading. Though there is a histerysis effect, it is important to point out that the loading/unloading curve is reversible. This fact is of primordial importance to build an analogy to plasticity.

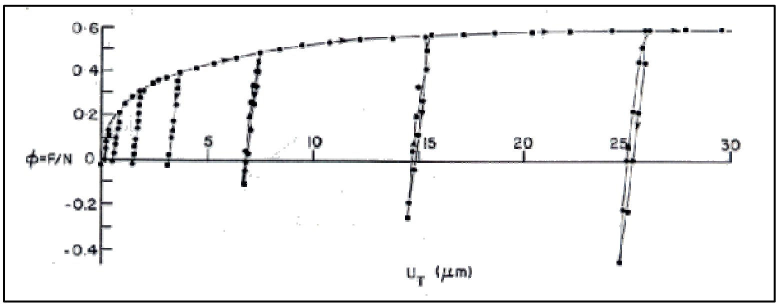

Figure 1: Courtney – Pratt and Eisner experiment

In what follows two terms, concerning frictional contact, namely adherence and slipping, will de adopted. The former is related to the reversible part of relative displacement in the interface, the elastic parallel, whereas the other addresses the part of displacement that is irreversible, and therefore related to dissipation in the interface, the inelastic component. It is supposed that interface relative displacement increments may be represented by means of the additive decomposition:

$$\Delta\bar{\mathbf{u}} = \Delta\bar{\mathbf{u}}^a + \Delta\bar{\mathbf{u}}^s; \quad \Delta\bar{\mathbf{u}} = \Delta\bar{\mathbf{u}}_n\mathbf{n} + \Delta\bar{\mathbf{u}}_i\mathbf{e}_i \quad i = 1,2 \tag{1}$$

where $\Delta\bar{\mathbf{u}} = \bar{\mathbf{v}}\Delta t$ is the increment of relative total displacement, with normal component $\Delta\bar{u}_n = \bar{v}_n\Delta t$; $\bar{v}_n = \bar{\mathbf{v}} \cdot \mathbf{n}\Delta\bar{\mathbf{u}}^a$ and tangential part $\Delta\bar{\mathbf{u}} = \Delta\bar{\mathbf{u}} - \Delta\bar{u}_n\mathbf{n} = \Delta\bar{u}_i\mathbf{e}_i$; $i = 1,2$ in the local basis $< \mathbf{n}, \mathbf{e}_1, \mathbf{e}_2 >$. Relative velocity between contactor body $B^+$and contacted body B^- is $\bar{\mathbf{v}} = \mathbf{v}^+ - \mathbf{v}^-$. The part of relative displacement in adherence is $\Delta\bar{u}^a$ while the part in slipping is $\Delta\bar{\mathbf{u}}^s$. Directions $i = 1,2$ correspond to tangential components of local basis $< \mathbf{n}, \mathbf{e}_1, \mathbf{e}_2 >$, which derives from global basis $< \mathbf{E}_1, \mathbf{E}_2, \mathbf{E}_3 >$by means of a basis rotation $\mathbf{R}$, used in the rate form as $\dot{\mathbf{R}}\mathbf{R}^T = \mathbf{\Omega}$ for the rate problem.

Related to the increments of displacement, instantaneous interface traction vector $\mathbf{t}$ components, that comprise normal $\mathbf{t}_n = t_n\mathbf{n}$ and tangential $\mathbf{t}_t = \mathbf{t} - t_n\mathbf{n} \quad t_i = \mathbf{t}\cdot\mathbf{e}_i; i = 1, 2$ parts, have increments:

$$\Delta\mathbf{t} = \Delta t_n\mathbf{n} + \Delta t_i\mathbf{e}_i; \quad \Delta t_n = \Delta\mathbf{t}\cdot\mathbf{n} \quad \Delta t_n^{\nabla} = -k_n\Delta\bar{u}_n \quad \Delta t_i^{\nabla} = -k_t\Delta\bar{u}_i^a \tag{2}$$

being $k_n > 0; k_t > 0$ interface scalar parameters for the stiffness in adherence. They may be functions of the pair$< \mathbf{t}, \alpha >$, being α a variable used to identify the state of the interface. According to experiments conducted by Courtney-Pratt and Eisner physically these parameters refer to the volumetric modulus and shear modulus at the interface, and here are taken to be constant.

2.2 Slipping condition

Interface slipping initiates whenever the magnitude of measure t_e^r of the relative interface tangential reaches a critical value r, related to the state of the surface. This value is the slipping resistance of the surface. Passage from the adherence condition to the slipping condition is set forth by function $f_c(\mathbf{t}, \mathbf{J}, r) \leq 0$, the subscript referring to contact. Vector $\mathbf{t} = t_1\mathbf{e}_1 + t_2\mathbf{e}_2$ represents tractions actuating at the contact point, whereas $\mathbf{J} = J_1\mathbf{e}_1 + J_2\mathbf{e}_2$ locates the center of the surface in the traction space. Scalar r has stress dimensions for unit area measures. Evolution of r is established by internal variables that characterize changes of frictional conditions during contact.

Function f_c has the general form:

$$f_c = t_e^r - r; \quad t_e^r = \sqrt{t_1^{r\,2} + t_2^{r\,2}}; \quad t_i^r = t_i - J_i, i = 1, 2; \quad r = \hat{r}(p, \bar{u}_e^s) \tag{3}$$

where t_e^r is the equivalent relative tangential traction. During loading/unloading two results are visualized: $f_c < 0$ when the pair of points in contact is in adherence and $f_c = 0$ when a neutral state is attained. Relative slipping measured by $\bar{\mathbf{u}}_e^s$ will take place concomitantly to the evolution of $r$surface. Pressure $p = -t_n$ is also an important variable for surface resistance measure.

2.3 Slipping rule and hardening

Once slipping is taking place in the tangential plane, normality for the deviatoric components may be supposed. Under such a hypothesis, components of relative displacement in slip obey:

$$\Delta\bar{u}_i^s = \Delta\lambda_c\frac{\partial F_c}{\partial t_i^r}; \quad t_i\mathbf{e}_i = \mathbf{t} - t_n\mathbf{n}; \quad i = 1, 2 \tag{4}$$

Figure 1 also shows another characteristic fact caused by the relative displacement between surfaces: There is a monotonic evolution of the curve, or in other words, resistance to slipping is constantly modified with the increase of the relative displacement. This behavior may be qualified as a typical case of hardening/softening of the interface as slipping takes place.

State of a material point in the interface at some instant t, is characterized by variable r and the instantaneous applied traction $\mathbf{t}$, relative to a reference position measured by variable $\mathbf{J}$. Essentially the constitutive model is a set of differential equations that describe the evolution of the triade $(\mathbf{t}, \mathbf{J}, r)$. Alterations in the slipping conditions at the interface are represented by means of internal variables. As pointed out by [4], one of the advantages of this formulation is that the model may be extended to other regimes of friction by choosing internal variables and forms of evolution of r.

One of the highest difficulties associated to this description is related to the modeling of the origin and evolution of the slip resistance. This difficulty comes from the complexity of the contact mechanics, involving deformation, fracture of rugosities, adhesion of fractured elements to new surfaces, presence of free particles and wear of the surfaces. Hence the slip resistance r is a function not only of the pressure, but the surface state variable α, $r = \hat{r}\,(p, \alpha)$, which needs to be specified in every case, by an adequate internal variable.

In the case of isotropic hardening, only a scalar variable needs to be considered, as the contact surface evolves with change of size, without change of form, or position. However when it comes to kinematic hardening, slip surface translation takes place. In the tangential traction space a vectorial variable is required to set the center of the surface. It resembles the backstress in plasticity. Both phenomena combined lead to a mixed model.

3 Constitutive law

3.1 Relative displacement decomposition

When an updated incremental Lagrange procedure is used, equilibrium is verified at discrete times. Configuration n, at time t is supposed known, i.e., $< \mathbf{t}, \mathbf{J}, \bar{\mathbf{u}}; s >$ is known, and the increment $\Delta\bar{\mathbf{u}}$ is available. In local coordinates, at the interface, $\bar{\mathbf{u}} = \bar{\mathbf{u}}_n \mathbf{n} + \bar{u}_i \mathbf{e}_i$ where $\bar{u}_i = \bar{u}_i^a + \bar{u}_i^s; i = 1, 2$. It is required the computation of the interface conditions at the next configuration, $n + 1$, corresponding to time $\tau = t + \Delta t$. When such a solution is obtained, then interface tractions and relative positions may be updated, as well as the surface resistance.

A contact interface model, derived from experimental evidences, was developed by [5] with diverse forms of evolution. If hardening supposes evolution of the surface in such a form that there is a size change and a migration of center, being this evolution independent of the rate of loading, it may be stated that::

$$\dot{r} = \frac{\partial r}{\partial p}\dot{p} + \frac{\partial r}{\partial \bar{u}_e^s}\dot{\bar{u}}_e^s; \quad r = \hat{r}(p, \bar{u}_e^s); \quad \bar{u}_e^s = \sqrt{\bar{u}_1^{s\,2} + \bar{u}_2^{s\,2}} \tag{5}$$

where $\bar{u}_e^s$ represents the accumulated relative slipping. In this way, considering the increment measured in between successive positions in the slipping surface, Eq. (3), it results from the consistency condition that:

$$\Delta f_c^{\nabla} = \frac{\partial f_c}{\partial t_1}\Delta t_1^{\nabla} + \frac{\partial f_c}{\partial t_2}\Delta t_2^{\nabla} + \frac{\partial f_c}{\partial J_1}\Delta J_1^{\nabla} + \frac{\partial f_c}{\partial J_2}\Delta J_2^{\nabla} + \frac{\partial f_c}{\partial r}\Delta r; \quad r = \hat{r}(\mu, s^*, p); \quad \Delta f_c = 0 \tag{6}$$

where:

$$\frac{\partial f_c}{\partial t_i} = \frac{t_i^r}{t_e^r} = \frac{t_i - J_i}{t_e^r} = m_i^r; \quad \frac{\partial f_c}{\partial J_i} = -m_i^r; i = 1, 2 \quad \wedge \frac{\partial f_c}{\partial r} = -1 \tag{7}$$

Mechanics of Solids in Brazil 2007, Marcílio Alves & H.S. da Costa Mattos (Editors)
Brazilian Society of Mechanical Sciences and Engineering, ISBN 978-85-85769-30-7

being $m_i^r = \hat{m}_i^r(\tau)$ the relative normal to the surface surf f_c, and

$$\Delta t_i^{\nabla} = -k_t \Delta \bar{u}_i^a; \quad \Delta \bar{u}_i^a = (\Delta \bar{u}_i - \Delta \bar{u}_i^s); \; \mathbf{t}^{\nabla} = \dot{\mathbf{t}} - \mathbf{\Omega t} \quad i = 1, 2. \tag{8}$$

the corotacional increment of the tangential components of traction. Moreover, the increment of interface resistance, derived from superficial hardening, and discarded any unloading, presents the increment:

$$\Delta r = \frac{\partial r}{\partial p} \Delta p + \frac{\partial r}{\partial \bar{u}_i^s} \Delta \bar{u}_i^s; \quad i = 1, 2 \quad \Delta p = k_n \Delta u_n; \; p = -t_n \tag{9}$$

that requires computation of components of relative displacement increment, Eq. (4);

$$\Delta \bar{\mathbf{u}}_i^s = \Delta \lambda_c \frac{\partial F_c}{\partial t_i}; \quad \Delta J_i^{\nabla} = \eta \Delta \bar{\mathbf{u}}_i^s; \quad i = 1, 2 \tag{10}$$

being η a constant, characteristic of the pair of surfaces in contact.

Therefore, substituting the above expressions into Eq. (6), it results the vectorial expression:

$$\Delta f_c = \mathbf{m}^r \cdot (\Delta \mathbf{t}^{r^{\nabla}} + \Delta \mathbf{\Omega} \mathbf{t}^r) - (\frac{\partial r}{\partial p} \Delta p + \frac{\partial r}{\partial \bar{\mathbf{u}}^s} \Delta \bar{\mathbf{u}}^s) \tag{11}$$

hence, once solved this equation, the relative multiplier of contact is, in the associative case, $F_c = f_c$:

$$\Delta \lambda_c = -\frac{k_t \mathbf{m}^r \cdot \Delta \bar{\mathbf{u}} + h_p \Delta p}{(k_t + \eta) + h_t \xi}; \quad \xi = \frac{\bar{u}_1^s}{\bar{u}_e^s} m_1^r + \frac{\bar{u}_2^s}{\bar{u}_e^s} m_2^r; \quad h_p = \frac{\partial r}{\partial p} \quad h_t = \frac{\partial r}{\partial \bar{u}_e^s} \tag{12}$$

Evaluation of this relation is, nonetheless, made difficult by the fact that the components of the unit tangential vector $\mathbf{m}^r$. For the tangential tractions it may also be stated that:

$$t_i^r(\tau) = t_i^r(t) + \Delta t_i^{r^{\nabla}} = t_i^r(t) - k_t[\Delta \bar{u}_i - \Delta \lambda_c m_i^r(\tau)] = t_i^{r^p}(\tau) + k_t m_i^r(\tau) \Delta \lambda_c \tag{13}$$

where the predictor $t_i^{r^p} = t_i^r - k_t \Delta \bar{u}_i$ was employed. Upon defining vector $\mathbf{m}^{r^p}$ according to:

$$m_i^{r^p} = \frac{t_i^{r^p}(\tau)}{t_e^{r^p}}; \quad t_e^{r^p}(\tau) = \sqrt{t_1^{r^p\,2} + t_2^{r^p\,2}} \tag{14}$$

and making substitution into Eq. (13) leads to

$$\mathbf{m}_r^p t_e^{r^p} = \mathbf{m}^r t_e^r + k_t \mathbf{m}^r \Delta \lambda_c \tag{15}$$

And then

$$\mathbf{m}^r = \omega^r \mathbf{m}^{r^p}; \quad \omega^r = \frac{t_e^{r^p}}{t_e^r + k_t \Delta \lambda_c} \tag{16}$$

Therefore $\omega^r = 1$, as both vectors used in the above expression are unitary. Thus, substitution of components of $\mathbf{m}^{r^p}$ into Eq. (12) allows computation of the increment of the contact multiplier λ_c.

3.2 Internal variables: updating

Once applied the above decomposition, the diverse variables may be updated. Obtained the new value of the relative tangential displacement, Eq. (10), updated values of the tractions may be obtained with Eq. (13). The same holds for the equivalent relative tangential displacement:

$$\bar{u}_e^s(\tau) = \bar{u}_e^s(t) + \Delta\bar{u}_e^s; \quad \Delta\bar{u}_e^s = \xi\Delta\lambda_c \tag{17}$$

Surface resistance update, in each particular form of equation, supposes updating several variables. If [6] form is considered, it results:

$$r = s^*(\bar{u}_e^s)tanh\left[\frac{\mu(\bar{u}_e^s)p}{s^*(\bar{u}_e^s)}\right] \tag{18}$$

dependent of the friction coefficient, saturation resistance and pressure. For the first:

$$\mu = \mu_0 + (\mu_s - \mu_0)[1 - \exp(-\bar{u}_e^s/\bar{u}_\mu); \quad \mu = \hat{\mu}(\bar{u}_e^s) \tag{19}$$

is supposed a function of three experimental variables $< \mu_0; \mu_s; \bar{u}_\mu >$; the other, the saturation resistance,

$$s^* = s_0^* + (s_s^* - s_0^*)[1 - \exp(-\bar{u}_e^s/\bar{u}_{s^*})]; \quad s^* = \hat{s}^*(\bar{u}_e^s) \tag{20}$$

again function of other triad of variables $< s_0^*; s_s^*; \bar{u}_{s^*} >$. Updating may be expressed again as:

$$\begin{aligned} &\mu(\tau) = \mu(t) + \Delta\mu \\ &\Delta\mu = h_\mu\Delta\bar{u}_e^s; \quad h_\mu = h_{\mu_0}\left[1 - \tfrac{\mu(\tau)}{\mu_S}\right]; \quad h_{\mu_0} = \tfrac{\mu_s}{\bar{u}_\mu} \end{aligned} \tag{21}$$

so that:

$$\mu(\tau) = \mu_S\frac{\mu(t) + h_{\mu_0}\Delta\bar{u}_e^s}{\mu_S + h_{\mu_0}\Delta\bar{u}_e^s} \tag{22}$$

Identically, updating of s^*, gathered all terms, produces:

$$s^*(\tau) = s^*(t) + \Delta s^*$$

$$\Delta s^* = h_{s^*}\Delta\bar{u}_e^s; \quad h_{s^*} = h_{s_0^*}\left[1 - \frac{s^*(\tau)}{s_s^*}\right]; \quad h_{s^*} = \frac{s_s^*}{\bar{u}_{s^*}} \tag{23}$$

so that:

$$s^*(\tau) = s_s^*\frac{s^*(t) + h_{s_0^*}\Delta\bar{u}_e^s}{s_s^* + h_{s_0^*}\Delta\bar{u}_e^s} \tag{24}$$

Evidently,

$$p(\tau) = p(t) + \Delta p \tag{25}$$

Algorithm

Normal tractions update:
$t_n^r(\tau) = t_n^r(t) - k_n \Delta\bar{u}_n; \quad \Delta\bar{u}_n = \Delta\bar{\mathbf{u}} \cdot \mathbf{n}$
Elastic predictor computation:
$\mathbf{t}^{r\,p^{\nabla}}(\tau) = \mathbf{t}^{r^{\nabla}}(t) + k_t \Delta\bar{\mathbf{u}}$
Adherence/Slip condition verification:
if
$t_e^{r\,p}(\tau) \le r(t)$ *adherence*
other
$t_e^{r\,p}(\tau) \ge r(t)$ *slipping.*
Find $\Delta\lambda_c$ *and update* $\Delta\bar{\mathrm{u}}_1^{\mathrm{s}}; \Delta\bar{\mathrm{u}}_2^{\mathrm{s}}$
Find $\Delta\bar{\mathrm{u}}_{\mathrm{e}}^{\mathrm{s}}$ *and compute*
$\mu(\tau)$ *e* $s^*(\tau)$
Find $r(\tau)$
Find radial return factor $rrf = \dfrac{r}{t_e^{r\,p}}$
Compute
$t_1^r = rrf * t_1^{r\,p}$ *and* $t_2^r = rrf * t_2^{r\,p}$
Find the Jacobian.
Return to solver in the main program.

3.3 Linearization modulus

The constitutive model presented above requires, for its implementation, that a linearization modulus be computed. Defining this modulus as:

$$\mathbf{M} = \partial_{\Delta\bar{\mathbf{u}}}\mathbf{t}^r; \quad \mathbf{t}^r = \mathbf{t} - \mathbf{J}; \quad \mathbf{t}^r = t_n^r\mathbf{n} + t_i^r\mathbf{e}_i; \quad \Delta\mathbf{u} = \Delta u_n\mathbf{n} + \Delta u_i\mathbf{e}_i; \quad i = 1,2 \tag{26}$$

computation may be readily done. Starting with Eq. (8) it is clear that,

$$\mathbf{t}^r = \mathbf{t}^{r^p} + k_t\mathbf{m}\Delta\lambda_c; \quad \mathbf{t}^r = \hat{\mathbf{t}}^r(\tau) \tag{27}$$

where,

$$t_n^{r^p} = t_n^r + k_n\Delta\bar{u}_n; \quad t_i^{r^p} = t_i^r + k_t\Delta\bar{u}_i; \quad i = 1,2 \tag{28}$$

represent the components of vector $\mathbf{t}^r$ at instant τ in terms of those components at instant t. From the decomposition $\mathbf{m}^r = m_n^r\mathbf{n} + m_i^r\mathbf{e}_i; \quad m_n^r = 0; \quad m_i^r = \frac{t_i^r}{t_e^r}$ it results that:

$$\mathbf{M} = \partial_{\Delta\bar{\mathbf{u}}}\mathbf{t}^{r^p} + k_t\Delta\lambda_c\partial_{\Delta\bar{\mathbf{u}}}\mathbf{m}^r + k_t\mathbf{m}\partial_{\Delta\bar{\mathbf{u}}}\Delta\lambda_c \tag{29}$$

First derivative above may be computed directly and it produces:

$$\mathbf{K} = k_n \mathbf{n} \otimes \mathbf{n} + k_t(\mathbf{I} - \mathbf{n} \otimes \mathbf{n}) \tag{30}$$

where $\mathbf{n} \otimes \mathbf{n}$ is the tensorial product of unit normal vectors and $\mathbf{I}$is the unit tensor of second order. In the same way, the second derivative above may be written as:

$$\partial_{\Delta \bar{\mathbf{u}}} \mathbf{m}^r = -\frac{k_t}{t_e^{r^p}} [\mathbf{I} - \mathbf{n} \otimes \mathbf{n} + \mathbf{m}^{r^p} \otimes \mathbf{m}^{r^p}] \tag{31}$$

once that $\mathbf{m}^r = \mathbf{m}^{r^p}$ as demonstrated above Last term of the above expression requires consideration of the resistance term, once $\Delta\lambda_c = \frac{t_e^{r^p} - r}{k_t}$, being $r = r(\mu, s^*, p)$. Therefore,

$$\partial_{\Delta \bar{\mathbf{u}}} \Delta\lambda_c = \mathbf{m}^{r^p} - \frac{1}{k_t} \partial_{\Delta \bar{\mathbf{u}}} r; \quad \partial_{\Delta \bar{\mathbf{u}}} r = \frac{\partial}{\partial \mu} \frac{\partial \mu}{\partial \Delta \bar{\mathbf{u}}} + \frac{\partial r}{\partial s^*} \frac{\partial s^*}{\partial \Delta \bar{\mathbf{u}}} + \frac{\partial r}{\partial p} \frac{\partial p}{\partial \Delta \bar{\mathbf{u}}} \tag{32}$$

Again, upon developing the required operations above, while dropping the r superscript:

$$\partial_{\Delta \mathbf{u}} \mu = \bar{h}_\mu \partial_{\Delta u_i} \Delta \bar{u}_e^s \mathbf{e_i}; i = 1, 2 \quad \bar{h}_\mu = \frac{h_\mu}{[1 - \frac{\partial h_\mu}{\partial \mu} \Delta \bar{u}_e^s]} \tag{33}$$

$$\partial_{\Delta \mathbf{u}} s^* = \bar{h}_{s^*} \partial_{\Delta u_i} \Delta \bar{u}_e^s \mathbf{e}_i; i = 1, 2 \quad \bar{h}_{s^*} = \frac{h_{s^*}}{[1 - \frac{\partial h_{s^*}}{\partial s^*} \Delta \bar{u}_e^s]} \tag{34}$$

$$\partial_{\Delta \mathbf{u}} p = -k_n \mathbf{n} \tag{35}$$

and combining the above results, it results for the first local direction,

$$\frac{\partial \Delta\lambda_c}{\partial \Delta u_1} = \frac{m_1^p - \frac{1}{k_t} \beta_1 \zeta \Delta\lambda_c}{1 + \frac{1}{k_t} \alpha \zeta}; \quad \beta_1 = \frac{\bar{u}_1^s}{\bar{u}_e^s} \left| \frac{\partial m_1^p}{\partial \Delta u_1} \right| + \frac{\bar{u}_2^s}{\bar{u}_e^s} \left| \frac{\partial m_2^p}{\partial \Delta u_1} \right| \tag{36}$$

being,

$$\alpha = \frac{\bar{u}_1^s}{\bar{u}_e^s} |m_1^p| + \frac{\bar{u}_2^s}{\bar{u}_e^s} |m_2^p|; \quad \zeta = \frac{\partial r}{\partial \mu} \bar{h}_\mu + \frac{\partial r}{\partial s^*} \bar{h}_{s^*} \tag{37}$$

whereas for the second direction, in a similar fashion it is obtained that:

$$\frac{\partial \Delta\lambda_c}{\partial \Delta u_2} = \frac{m_2^p - \frac{1}{k_t} \beta_2 \zeta \Delta\lambda_c}{1 + \frac{1}{k_t} \alpha \zeta}; \quad \beta_2 = \frac{\bar{u}_1^s}{\bar{u}_e^s} \left| \frac{\partial m_1^p}{\partial \Delta u_2} \right| + \frac{\bar{u}_2^s}{\bar{u}_e^s} \left| \frac{\partial m_2^p}{\partial \Delta u_2} \right| \tag{38}$$

so that, with the simple addition of the above results, the expression for $\mathbf{M}$ is obtained.

4 Results

4.1 Model verification

Magnitude of slipping determines evolution of surface resistance. Furthermore the way relative motion evolves changes the tractions required to produce them. In order to verify these facts, a numerical experiment comprising motion of a block, in different directions, named 1 and 2, is performed. The block with squared sectional form, with unit dimensions, is displaced in a quasi-static manner from initial position $< 0.; 0. >$ till position $< 2.0; 1.0 >$ in the first step. Next it is returned to initial position. It is expected that tractions in directions 1 and 2 be different, as the displacements have different amplitudes. As displacement in direction 1 is larger than that of direction 2, contact surface should suffer hardening in an amount larger in this direction, and thus develop greater tractions.

Results shown in figures 2 and 3 demonstrate these assertions. Higher values of traction are obtained in direction 1: about twice the values for direction 2. In these plots, Bauschinger effect, in both directions, is also present.

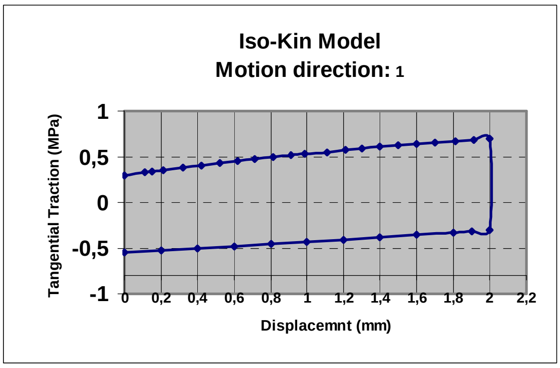

Figure 2: Tractions in direction 1

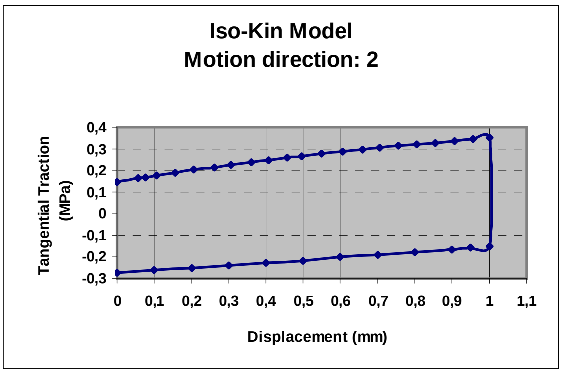

Figure 3: Tractions in direction 2

4.2 Application

Extrusion, figure 4, is an appropriate process to use in a simulation of a constitutive interface law because friction is the most important dissipation mechanism in this process, figure 5. Here, a tool displacement of 6 mm, axial, is applied to the loading cylinder, located in the lower side of the figure. Friction occurs in the side walls contact with the container die. The interface model shown above, supposing isotropic behavior, using 240 axis-symmetric four noded elements, is used in the solution. Large displacements and strains occur, so that a non-linear incremental formulation is used. Processor of the finite element program Abaqus was used in this endeavor, [7].

In the plot of figure 6, evolution of the reaction force, axial, with respect to the displacement of the loading cylinder is shown. Model variables were assumed to value: $< \mu_0 = 0,33; \mu_s = 0,577; s_0^* = 108; s_s^* = 220 >$, with $h_{\mu_0} = 0,418; h_{s_0^*} = 44$. Cooper OFHC was the material under extrusion. Coulomb model was also used to compare results. Four values of friction were considered in the problem; graph colors identify these cases. Friction coefficients considered were $\mu = 0.33$, for the green color, μ= 0.577 for the blue. Average value $\mu = 0,45$, yellow color, was also employed. Hardening limits were set to μ_0 and μ_s. Normal parameters were also changed in the analysis. Lower normal stiffness κ_n was identified with the yellow color, model 1, and a larger normal stiffness related to the orange color, model 2. Experimental results, used in the verification of the model, are shown in red.

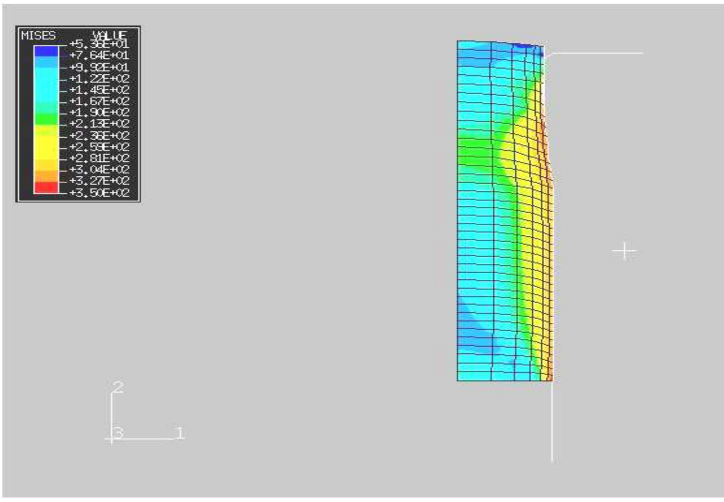

displacement [mm]

Figure 4: Deformed position and stress field in extrusion problem

Isoentropic hardening used in the above case was considered as a means of approaching the Coulomb model. Results show that model results, red, and experimental ones, green, agree very closely.

5 Conclusions

Qualitative solutions, obtained with implementation of the above model, are in agreement with the expected. Accepting an isotropic evolution of the friction surface, however, only allows modeling of non-cyclic motions. Adoption of the combined model, iso-kinematic model, does permit this kind of motion to be considered. Indeed obtained results reveal difference of behavior. Presence of Bauschinger effect in the transition of the direction of motions is produced, as experimental evidence also confirms.

Mechanics of Solids in Brazil 2007, Marcílio Alves & H.S. da Costa Mattos (Editors)
Brazilian Society of Mechanical Sciences and Engineering, ISBN 978-85-85769-30-7

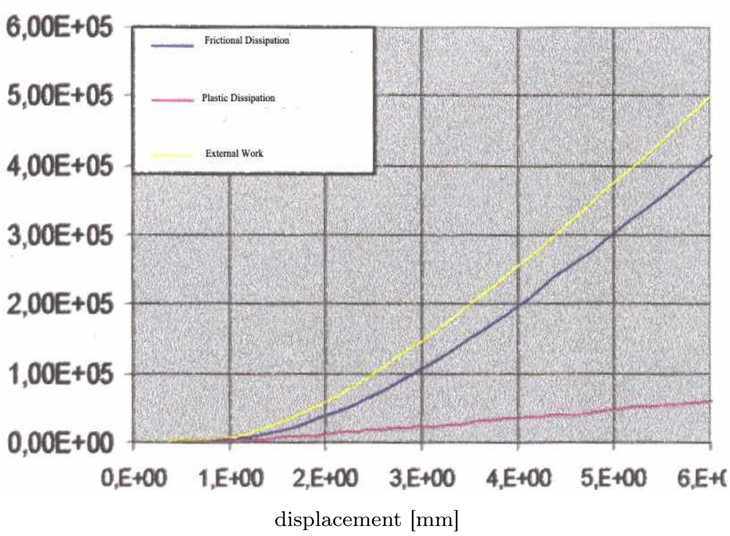

Figure 5: Energy partition in extrusion problem

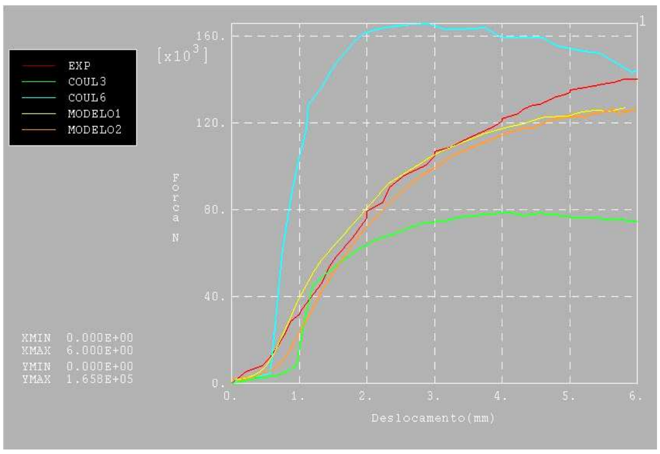

Figure 6: Reaction forces under different frictional models

The description presented here may be extended by considering temperature as well as rate dependence. In this case, the appropriate form of this dependence, obtained in experimental form, would be required. Moreover, in some occasions it is advocated the necessity of using a nonlinear stiffness description. This can also be tried here, without major problems.

References

[1] Wriggers, P., *Computational Contact Mechanics*. John Wiley & Sons: England, 2002.
[2] Curnier, A., A theory of friction. *Int J Solids Structures*, **20(7)**, pp. 637–647, 1984.
[3] Courtney-Pratt, J.S. & Eisner, E., (eds.), *The Effect of Tangential Force on the Contact of Metallic Bodies*, volume 238, Royal Society, 1957.
[4] Pisoni, A., *A Constitutive Model for Friction in Metal-Working*. Master's thesis, M.I.T., 1993.
[5] Tong, W. & Anand, L., A constitutive model for friction in forming. *Annals of the CIRP*, **42**, pp. 361–366, 1993.
[6] Bay, N., Wanheim, T. & Avitzur, B., Models for friction in metal forming. *Manufacturing Technology Review*, **2**, pp. 372–378, 1987.
[7] Vargas, R.T., *Formulação e Implementação de uma Lei Constitutiva de Atrito*. Ph.D. thesis, EPUSP, 2003.

Mechanics of Solids in Brazil 2007, Marcílio Alves & H.S. da Costa Mattos (Editors)
Brazilian Society of Mechanical Sciences and Engineering, ISBN 978-85-85769-30-7